

FEDSM2002-31047

**ACTIVE CONTROL OF SEPARATION BUBBLES EXPLOITING LAMINAR
 BASEFLOW INSTABILITIES**

Kai Augustin*

Institut für Aerodynamik und Gasdynamik
 Universität Stuttgart
 D-70550 Stuttgart
 Germany
 Email: augustin@iag.uni-stuttgart.de

Ulrich Rist†

Siegfried Wagner‡
 Institut für Aerodynamik und Gasdynamik
 Universität Stuttgart
 D-70550 Stuttgart
 Germany
 Email: rist@iag.uni-stuttgart.de
 Email: wagner@iag.uni-stuttgart.de

ABSTRACT

In the present paper laminar separation bubbles are investigated by means of direct numerical simulations with respect to steady and unsteady 2D and 3D *Tollmien-Schlichting* (TS) like boundary layer disturbances. The specific influence of several disturbance modes on the size and shape of the laminar separation bubble are considered to allow for an effective reduction of the region of separated flow. Based on these results a criterion to detect the extension of the bubble is derived which is a suitable input for a controller.

NOMENCLATURE

f Disturbance frequency [Hz]
 h Index denoting higher harmonics of the fundamental disturbance frequency
 i imaginary unit = $\sqrt{-1}$
 k Index denoting multiples of the spanwise wavenumber
 u Streamwise velocity
 v Wall-normal velocity
 w Spanwise velocity
 x Streamwise spatial coordinate
 y Wall-normal spatial coordinate

z Spanwise spatial coordinate
 A_0 Initial disturbance amplitude
 C Binary bubble criterion
 N Accumulated number of points
 Re_{δ_1} Momentum thickness Reynolds number = $\frac{U_\infty \delta_1}{\nu}$
 L Reference length [m]
 U_∞ Freestream velocity [m/s]
 α_r Streamwise wavenumber
 β Angular frequency of the disturbance
 γ Spanwise wavenumber
 δ_1 Momentum thickness [m]
 λ_z Spanwise wavelength
 ν Kinematic viscosity [m^2/s]
 ω_z Streamwise vorticity
 ω_y Wall-normal vorticity
 ω_z Spanwise vorticity
 $\omega_{z,wall}$ Skin friction
 Ψ_0 Separation stream-surface
 $\bar{\Psi}_0$ Time and spanwise averaged separation streamline
 $\tilde{\Delta}$ Modified Laplace Operator
 \wedge Dimensional variables
 $'$ Non-dimensional disturbance velocities

INTRODUCTION

Adverse pressure gradient (APG) boundary layers at low

*Research Assistant
 †Senior Research Scientist
 ‡Professor, Institute Director

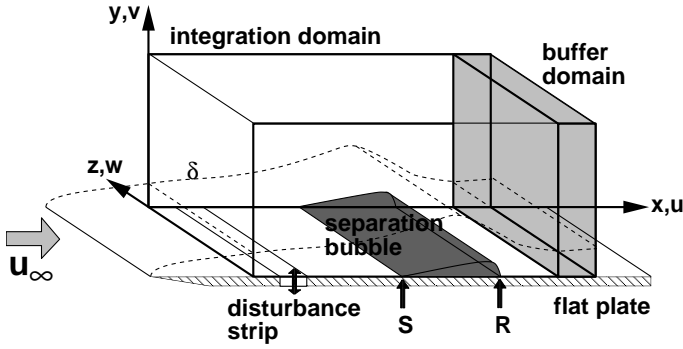


Figure 1. DNS 3D INTEGRATION DOMAIN WITH SEPARATION BUBBLE AND DISTURBANCE STRIP. "S" MARKS THE POINT OF SEPARATION AND "R" THE POINT OF REATTACHMENT.

Reynolds numbers are strongly susceptible to laminar separation. Due to the deceleration of the flow the laminar boundary layer separates from the surface, laminar-turbulent breakdown occurs at a certain distance from the separation line and the now turbulent flow reattaches subsequently. The area of reverse flow and therefore negative skin friction between separation and reattachment is called a *laminar separation bubble* (LSB) or alternatively transitional separation bubble, because of the laminar-turbulent transition occurring. Despite the effect of lowering the skin friction within the bubble the LSB has a considerable influence on the global pressure distribution of the airfoil and causes an undesired drag rise.

NUMERICAL MODEL

To investigate laminar separation bubbles spatial *direct numerical simulations* (DNS) of a flat plate boundary layer with a 2D baseflow and an applied APG at the freestream boundary are performed. The DNS code has been used in different research programs for the investigation of transitional boundary layers in both disturbance and total-flow formulation (Kloker, 1993; Rist, Fasel, 1995). Figure 1 shows a sketch of the rectangular integration domain. The complete Navier-Stokes equations for incompressible flow are solved in a vorticity-velocity formulation as given in equation (1).

$$\begin{aligned}
 \frac{\partial \omega_x}{\partial t} + \frac{\partial}{\partial y} (v\omega_x - u\omega_y) + \frac{\partial}{\partial z} (w\omega_x - u\omega_z) &= \tilde{\Delta} \omega_x \\
 \frac{\partial \omega_y}{\partial t} + \frac{\partial}{\partial x} (u\omega_y - v\omega_x) + \frac{\partial}{\partial z} (w\omega_y - v\omega_z) &= \tilde{\Delta} \omega_y \\
 \frac{\partial \omega_z}{\partial t} + \frac{\partial}{\partial x} (u\omega_z - w\omega_x) + \frac{\partial}{\partial y} (v\omega_z - w\omega_y) &= \tilde{\Delta} \omega_z
 \end{aligned} \quad (1)$$

Once the vorticity-transport equations are solved the remaining velocity components can be computed from three Poisson equations (2).

$$\begin{aligned}
 \frac{\partial^2 u}{\partial x^2} + \frac{\partial^2 u}{\partial z^2} &= -\frac{\partial \omega_y}{\partial z} - \frac{\partial^2 v}{\partial x \partial y} \\
 \tilde{\Delta} v &= \frac{\partial \omega_x}{\partial z} - \frac{\partial \omega_z}{\partial x} \\
 \frac{\partial^2 w}{\partial x^2} + \frac{\partial^2 w}{\partial z^2} &= \frac{\partial \omega_y}{\partial x} - \frac{\partial^2 v}{\partial y \partial z}
 \end{aligned} \quad (2)$$

Non-dimensionalization is done by referencing to the free stream velocity $\hat{U}_\infty = 30 \text{ m/s}$, a characteristic length $\hat{L} = 0.05 \text{ m}$ and the kinematic viscosity $\hat{\nu} = 15 \cdot 10^{-6} \text{ m}^2/\text{s}$. Thus the non-dimensional variables (3) and a modified Laplace operator (4) can be derived.

$$\begin{aligned}
 Re &= \frac{\hat{U}_\infty \hat{L}}{\hat{\nu}} & \beta &= \frac{2\pi \hat{f} \hat{\nu} Re}{\hat{U}_\infty^2} \\
 x &= \frac{\hat{x}}{\hat{L}} & y &= \sqrt{Re} \frac{\hat{y}}{\hat{L}} & z &= \frac{\hat{z}}{\hat{L}} \\
 u &= \frac{\hat{u}}{\hat{U}_\infty} & v &= \sqrt{Re} \frac{\hat{v}}{\hat{U}_\infty} & w &= \frac{\hat{w}}{\hat{U}_\infty}
 \end{aligned} \quad (3)$$

$$\tilde{\Delta} = \frac{1}{Re} \frac{\partial^2}{\partial x^2} + \frac{\partial^2}{\partial y^2} + \frac{1}{Re} \frac{\partial^2}{\partial z^2} \quad (4)$$

A 4th-order accurate numerical method is applied in time and space by finite differences in streamwise and wall-normal direction and by a Runge-Kutta scheme in time. For the spanwise direction a spectral ansatz (5) implying periodic boundary conditions is used.

$$f(x, y, z, t) = \sum_{k=-K}^K F_k(x, y, t) \cdot e^{ik\gamma z}, \quad \gamma = \frac{2\pi}{\lambda_z} \quad (5)$$

Due to the spectral ansatz the Poisson equations for the streamwise and spanwise velocity reduce to ordinary differential equations. The remaining Poisson equation for the wall normal velocity is solved by a line relaxation method using a multigrid algorithm. All Poisson equations can be solved separately for each spanwise spectral mode k allowing effective parallelization. At the inflow boundary a Blasius boundary layer solution with $Re_{\delta_1} = 1722$ is prescribed. To avoid non-physical reflections at the outflow boundary the disturbance amplitudes are artificially damped in a buffer domain (Kloker et al., 1993) by several orders of magnitude. The potential flow at the freestream upper boundary is decelerated by 10% of \hat{U}_∞ and the displacement effects of the LSB on the potential flow are captured by a viscous-inviscid

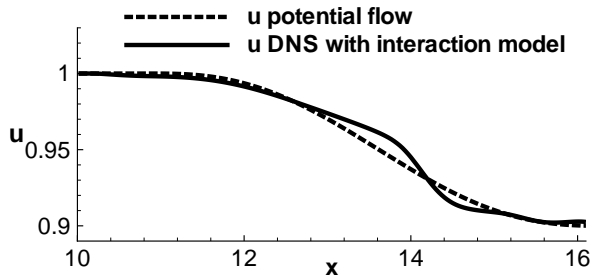


Figure 2. STREAMWISE FREESTREAM BOUNDARY CONDITION WITH POTENTIAL DISTRIBUTION AT THE STARTUP OF THE DNS AND THE DISTRIBUTION DEVELOPING FROM THE INTERACTION MODEL

boundary layer interaction model (Maucher et al., 2000) at every timestep of the calculation. In Figure 2 the resulting streamwise velocity distribution at the upper boundary as a result from the interaction model is compared to the initial potential flow prescribed at the startup of the computation. The characteristic “pressure plateau” formed by the LSB is clearly visible from the solid line distribution. On the surface of the plate the no-slip condition is applied. At a disturbance strip arbitrary 2D and 3D boundary layer disturbances can be introduced into the flow by suction and blowing at the wall upstream of the LSB.

DISTURBANCE DEVELOPMENT

To successfully control the size of a LSB via the adjustment of the transition location, knowledge of the influence of different disturbance parameters on the bubble is elementary. This includes insight into the stability mechanisms of the base flow and into the resulting amplification or damping effect on boundary layer disturbances. As a constraint, these properties can be used to minimize the necessary kinetic energy to be introduced into the flow by an actuator. Another focus has to be set on the identification of the bubble by a sensor system and a criterion which facilitates control of the LSB. For these investigations a midchord bubble case described in much detail in (Rist, 1999) is used. Following 2D investigations by DNS and linear stability theory (Augustin et al., 2000; Rist et al., 2002), the scope has been extended to 3D disturbances in the mean time. Primary parameters for the specification of disturbances are amplitude A_0 , frequency β and their streamwise and spanwise wavenumbers α_r and γ , respectively.

The results show a different behavior of the LSB with respect to steady and unsteady disturbances. Figure 3 compares amplification curves of the disturbance velocity u' versus x for different 2D and 3D spectral modes in logarithmic scale. The position of the disturbance strip as well as the points of separation

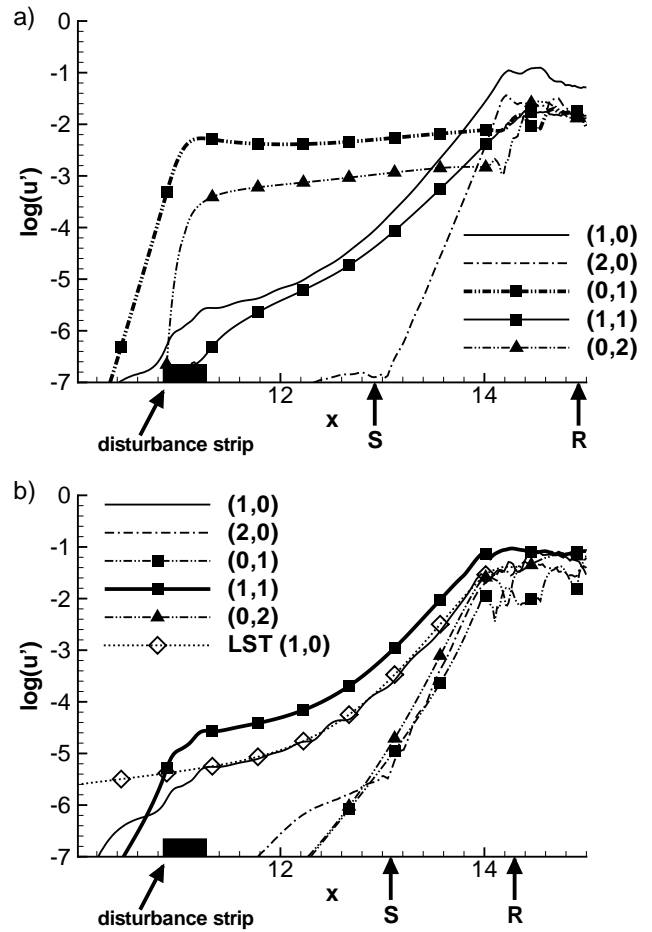


Figure 3. AMPLIFICATION CURVE OF THE DISTURBANCE VELOCITY u' OF 2D AND 3D DISTURBANCES FOR THE A) STEADY CASE AND THE B) OBLIQUE UNSTEADY CASE.

tion “S” and reattachment “R” are marked.

Steady 3D Case

In the first case a steady 3D disturbance mode (0,1) (bold dash-dot-dotted line with squares) is excited at the disturbance strip with a wall-normal amplitude $v'_{(0,1)} = 10^{-3}$. Further on, this case will be referred to as the “steady case”. In the notation (h,k) the index h denotes harmonic modes with multiples of the fundamental frequency β (equation (3)) while k means spectral modes of the spanwise wavenumber γ (equation (5)). Thus (0,1) stands for a steady 3D disturbance with a spanwise wavelength $\lambda_z = 0.419$. Advancing in downstream direction the disturbance amplitude of mode (0,1) is weakly damped at first and then weakly amplified far into the bubble. Only at $x \approx 14.2$ it grows close to the point of non-linear saturation which marks the

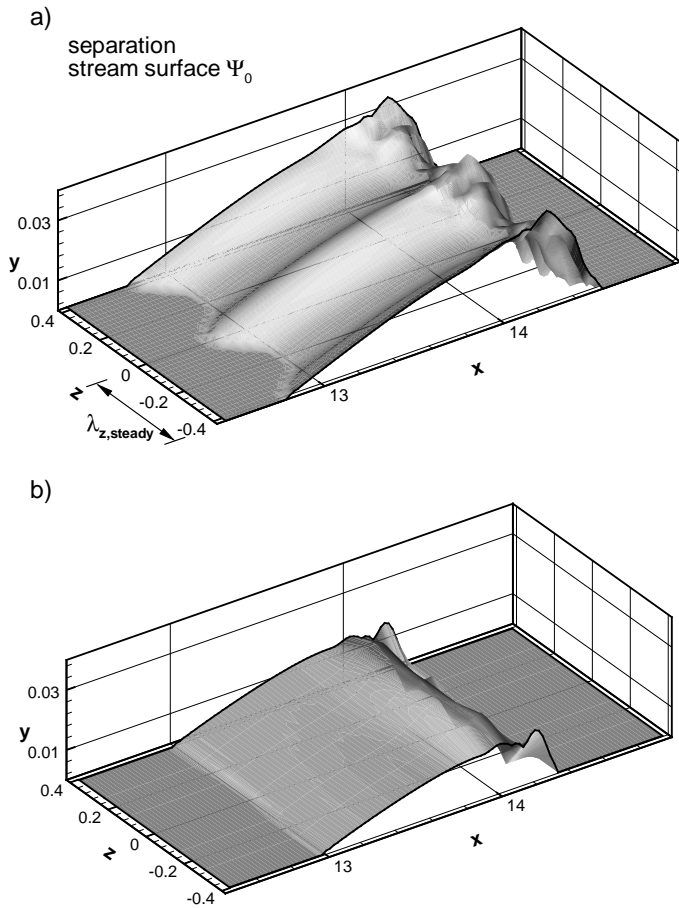


Figure 4. SEPARATION STREAM SURFACE Ψ_0 FOR THE A) STEADY CASE AND THE B) OBLIQUE UNSTEADY CASE.

transition. A higher spanwise harmonic mode (0,2) (dash-dot-dotted line with deltas) is generated by non-linear interaction of the mode (0,1) with itself. At the disturbance strip an additional 2D mode (1,0) (solid line) of fundamental frequency has been excited to mimic background disturbances with an initial amplitude $v'_{(1,0)} = 10^{-6}$, three orders of magnitude below the amplitude of the 3D mode (0,1). This TS mode becomes strongly amplified by baseflow instability and exceeds the amplitude of the 3D mode (0,1) at $x = 13.8$. It supersedes the steady mode (0,1) as the most dominant disturbance. An oblique fundamental mode (1,1) is generated by nonlinear interaction of the (1,0) and (0,1) modes continuously and finally reaches the amplitude of the 3D steady mode. The whole scenario is dominated by unsteady 2D effects and three dimensionality plays only a minor role. Figure 4 a) shows the 3D modulation of the separation stream surface Ψ_0 with the spanwise wavelength of mode (0,1), as marked by $\lambda_{z,steady}$, of the otherwise 2D LSB. The separa-

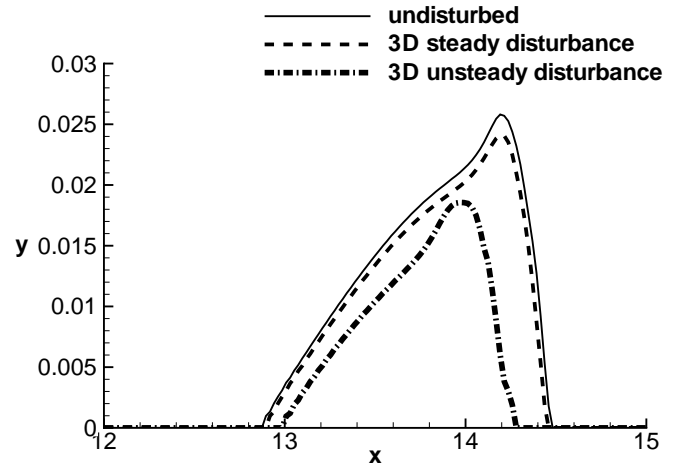


Figure 5. OUTLINE OF THE SEPARATION BUBBLES OF THE THREE DIFFERENT CASES BY THE TIME AND SPACE AVERAGED SEPARATION STREAMLINE $\bar{\Psi}_0$

tion stream surface Ψ_0 is defined as the value of the y -coordinate where the stream function $\Psi = \Psi(x, y, z)$ becomes zero.

Purely Oblique Unsteady 3D Case

In a second scenario an oblique (10°) unsteady mode (1,1) only (bold solid line with squares in figure 3 b)) is introduced into the same base flow as before. This case will be referred to as the “oblique unsteady case”. The initial disturbance amplitude of mode (1,1) has been set to $v'_{(1,1)} = 10^{-5}$ at the wall. Figure 3 b) shows the disturbance development in this second case. Again an unsteady 2D background disturbance (1,0) (solid line) is also present with the same initial amplitude $v'_{(1,0)} = 10^{-6}$ as before. For verification purposes the development of the 2D mode (1,0) is compared to linear stability theory. Due to its very low amplitude even inside the LSB the mode shows very good agreement with the theory up to saturation.

In contrast to the first case the wall-forced unsteady TS mode (1,1) is strongly amplified by boundary layer instability and continues to be the most dominant mode. Although equally amplified, the 2D mode (1,0) stays below the oblique one due to the lower initial amplitude. Because of the strong amplification of mode (1,1) non-linear stages of the disturbance development ($\approx 1\% \hat{U}_\infty$) are reached somewhat further upstream than in the “steady case” at $x = 14.0$. The point of laminar-turbulent transition and thus the reattachment is shifted upstream likewise. Figure 4 b) shows this effect again by the separation stream surface Ψ_0 . Compared to the large one in Figure 4 a) the LSB is much shorter, of lower height and only slightly modulated in spanwise direction. Additional simulations show that the bubble vanishes totally at an initial disturbance level of $v'_{(1,1)} = 10^{-3}$.

Comparison

The difference in size of the bubble can also be compared by the time and spanwise averaged separation streamlines $\bar{\Psi}_0$ in figure 5. The strong influence of unsteady modes is even more obvious here. Both cases are compared to an undisturbed third case (solid line), where only small background disturbances are present in the flow. In the “steady case” (dashed line) the shape and size of the bubble merely differs from the undisturbed case, whereas in the “oblique unsteady case” (bold dash-dotted line) the height is only 72% and the length only 76% of the undisturbed bubble. This is valid despite the fact that the initial disturbance amplitude of the (0,1)-mode in the “steady case” is a hundred times larger than the amplitude of the (1,1)-mode in the “oblique unsteady case”. At small angles of obliqueness the effect of 3D unsteady modes is similar to the behavior of 2D unsteady modes (Rist et al., 2002). This clearly shows the superiority of unsteady control to steady control.

BUBBLE CONTROL

The above results led us to a mechanism to automatically control flows with laminar separation bubbles. It requires the measured size of the LSB to adjust the amplitude upstream at the disturbance strip. One way to determine the length of a LSB is based on the time averaged skin friction $\omega_{z,wall}$.

Figure 6 shows the time averaged ω_z as contours at the wall for the two cases considered above. The attached flow upstream of the separation marked by positive values of $\omega_{z,wall}$ can be observed, as well as spanwise periodic structures inside and outside the LSB. The contour table is chosen to emphasize the separation and reattachment line where $\omega_{z,wall}$ becomes zero. It makes the streamwise position of the separation line easy to detect, although it is modulated in spanwise direction by λ_z of the steady (0,1)-mode as shown in figure 6 a). Unlike the separation the reattachment is hidden in an area of large gradients of the skin friction caused by a leftover from the highly unsteady processes connected to large amplitude vortex shedding in the reattachment region of the separation bubble. To resolve this problem one can use histograms of the spanwise skin friction at discrete streamwise positions to derive a clearer and easy-to-implement bubble detection criterion. In those histograms $\omega_{z,wall}$ is decomposed into intervals. Values within the same interval are counted and finally normalized by the total number of analyzed points N . Time averaging is done by performing this analysis for all timesteps over a fixed period of time. In the present study 4 periods of the fundamental disturbance frequency are used. The upper row of plots in figure 7 contains histograms for eleven intervals in the range $-0.1 \leq \omega_{z,wall} \leq 0.1$ at three x -positions. At the first streamwise position $x = 13.58$ (also marked in figure 6 b) as a dashed line) the histogram shows a sharp peak at weakly negative values. This obviously belongs to a position inside the separation bubble. Going further downstream this peak is smeared

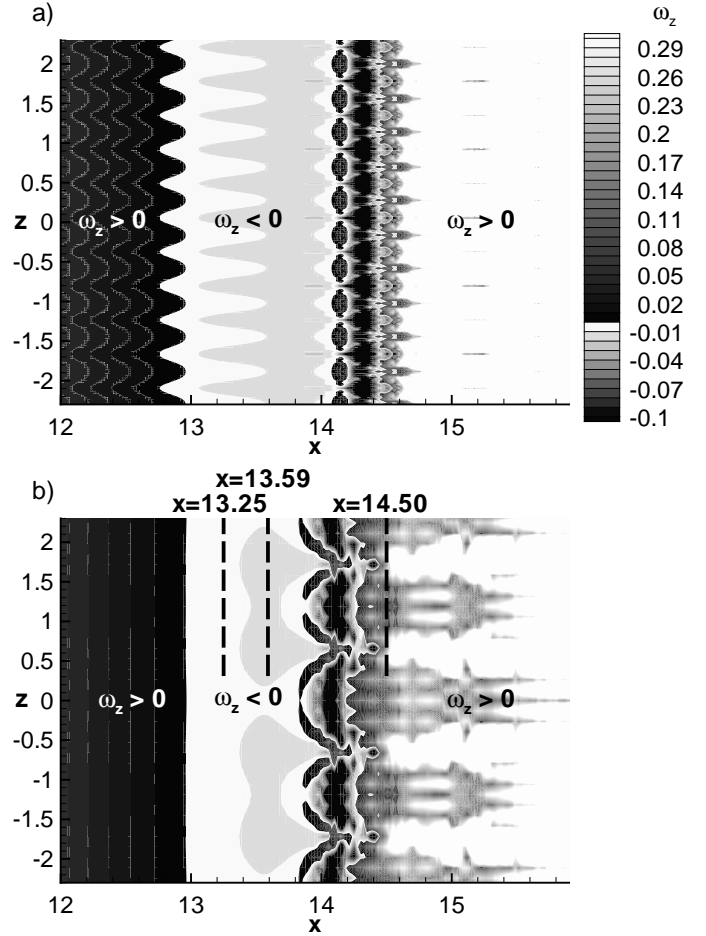


Figure 6. TIME AVERAGED SKIN FRICTION $\omega_{z,wall}$ FOR A) THE STEADY AND B) THE OBLIQUE UNSTEADY CASE

out more and more and it is hardly possible to decide whether a point inside or outside the bubble is encountered. Another simplification can provide a clearer view by restricting the analysis to only two intervals of $\omega_{z,wall}$, one below and one above zero, as illustrated in the lower row of figure 7. If the number N of points with $\omega_{z,wall}$ values below zero exceeds the number of points with $\omega_{z,wall}$ values larger than zero, the considered streamwise position lies within the bubble. These properties can be used to define a binary separation bubble criterion

$$C_{\omega_{z,wall}}(x) = \begin{cases} 1 & N_{\omega_{z,wall} < 0} \leq N_{\omega_{z,wall} > 0} \\ 0 & N_{\omega_{z,wall} < 0} > N_{\omega_{z,wall} > 0} \end{cases}, \quad (6)$$

which becomes 1 for points located inside the bubble and 0 for all other streamwise points. Applied to the undisturbed case, the “steady case” and the “oblique unsteady case”, the extension of

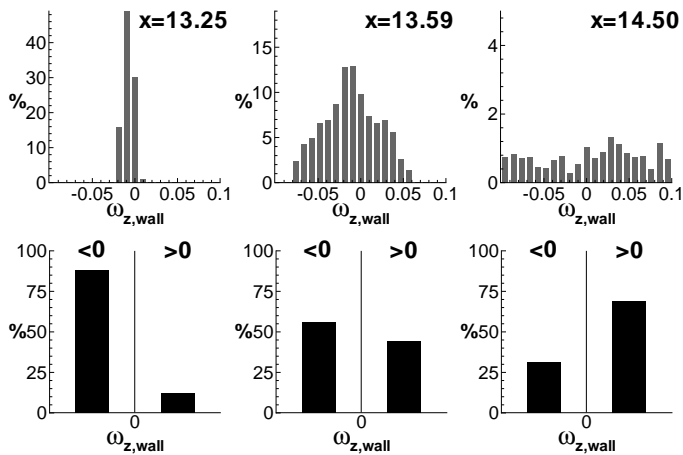


Figure 7. HISTOGRAMS OF THE SPANWISE DISTRIBUTION OF THE SKIN FRICTION $\omega_{z,wall}$ AT THREE STREAMWISE POSITIONS FOR THE OBLIQUE UNSTEADY CASE.

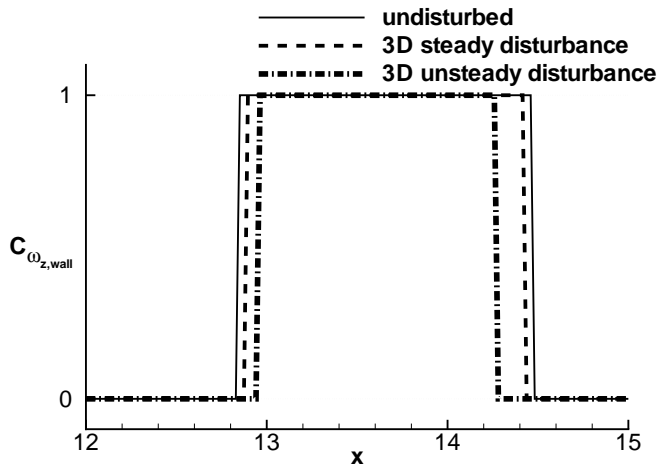


Figure 8. EXTENT OF THE SEPARATION BUBBLES OF THE THREE DIFFERENT CASES AS DETECTED BY THE BINARY BUBBLE CRITERION $C_{\omega_{z,wall}}(x)$.

the respective LSB can be confidently determined by the above criterion (compare figure 5 and figure 8). However, a shortcoming of this easy-to-use method is that only the streamwise extension but not the height of the LSB can be used for the control of the bubble. Sometimes a long but shallow separation is desired because of the low skin friction inside the bubble leading to a lowering of the total drag. Nevertheless, the bubble criterion is well suited for a controller which then changes the amplitude of the disturbance input upstream and thus reduces the LSB.

CONCLUSIONS

Laminar separation bubbles have been investigated by means of direct numerical simulations in an adverse pressure gradient flow over a flat plate. Different steady and unsteady boundary layer disturbances were introduced by a disturbance strip upstream of the separation and their effects on the separation bubble have been studied. 2D or weakly 3D unsteady disturbances have a stronger impact on the size of the bubble than steady disturbances by utilizing baseflow instability. An initial amplitude for an unsteady 2D or 3D disturbance two to three orders of magnitude lower than a steady disturbance is sufficient to gain the same or a even larger effect on the LSB.

The effect of different kinds of disturbances on separation bubble control can confidently be evaluated by an easy-to-implement binary separation bubble criterion based on discrete values of the skin friction. The criterion will be used as input for an active control mechanism for separation bubble flows.

ACKNOWLEDGMENT

This project is supported by the *Deutsche Forschungsgemeinschaft* (German Research Foundation, DFG) under project number Ri 680/11-1.

REFERENCES

- Augustin, K., Rist, U. & Wagner, S., *Active Control of a Laminar Separation Bubble*, Aerodynamic Drag Reduction Technologies, Notes on Numerical Fluid Mechanics (NNFM), Vol. 76, pp. 297-303, Springer, 2001.
- Kloker, M., *Direkte numerische Simulation des laminar-turbulenten Strömungsumschlags in einer stark verzögerten Grenzschicht*, Dissertation, Universität Stuttgart, 1993.
- Kloker, M., Konzelman, U. & Fasel, H., *Outflow Boundary Conditions for spatial Navier-Stokes Numerical Simulations of Transition Boundary Layers*, AIAA Journal, Vol. 31(4), pp. 620-628, 1993.
- Maucher, U., Rist, U. & Wagner, S., *Refined Interaction Method for Direct Numerical Simulation of Transition in Separation Bubbles*, AIAA Journal, Vol. 38(8), pp. 1385-1393, 2000.
- Rist, U. & Fasel, H., *Direct Numerical Simulation of Controlled Transition in a Flat-Plate Boundary Layer*, J. Fluid Mech., 298:211-248, 1995.
- Rist, U., *Zur Instabilität und Transition in laminaren Ablöseblasen*, Habilitation, Universität Stuttgart, Shaker-Verlag, 1999.
- Rist, U., Augustin, K. & Wagner, S., *Numerical Simulation of Laminar Separation-Bubble Control*, New Results in Experimental and Computational Fluid Dynamics III, Notes on Numerical Fluid Mechanics (NNFM), Vol. 77, pp. 170-177, Springer, 2002.